

OUTSIZED CONTRIBUTION OF THE SEMI-ARID ECOSYSTEMS TO INTERANNUAL VARIABILITY IN NORTH AMERICAN ECOSYSTEMS

Brendan Byrne^{1*}, Junjie Liu², A. Anthony Bloom², Kevin W. Bowman², Zachary Butterfield³, Joanna Joiner⁴, Trevor F. Keenan^{5,6}, Gretchen Keppel-Aleks³, Nicholas C. Parazoo², and Yi Yin⁷

¹NASA Postdoctoral Program Fellow, Jet Propulsion Laboratory, California Institute of Technology, CA, USA

²Jet Propulsion Laboratory, California Institute of Technology, CA, USA

³Department of Climate and Space Sciences and Engineering, University of Michigan, Ann Arbor, MI, USA

⁴Goddard Space Flight Center, Greenbelt, MD 20771, USA

⁵Earth and Environmental Sciences Area, Lawrence Berkeley National Laboratory, Berkeley, California, USA

⁶Department of Environmental Science, Policy and Management, University of California, Berkeley, Berkeley, California, USA

⁷Division of Geological and Planetary Sciences, California Institute of Technology, Pasadena, CA, USA

*brendan.k.byrne@jpl.nasa.gov

BACKGROUND

- Over the past 60 years, flask and in situ CO_2 measurements at surface sites have revealed large scale features of the global carbon cycle.
- Driven by increasing observational density, much of the current top-down research emphasizes estimating surface-atmosphere CO_2 fluxes on smaller spatial and temporal scales.

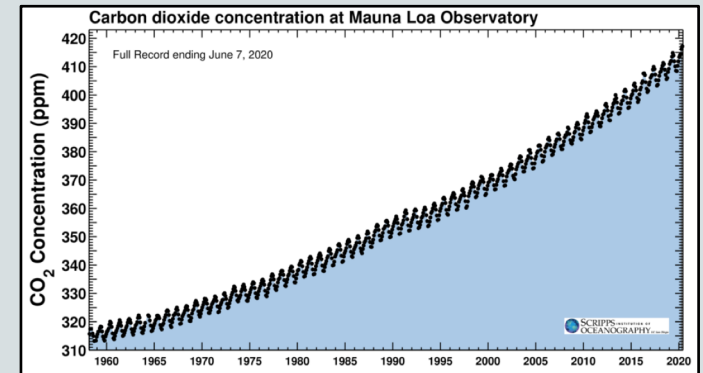


Figure 1. CO_2 measured at Mauna Loa, Hawaii (Keeling et al., 2001).

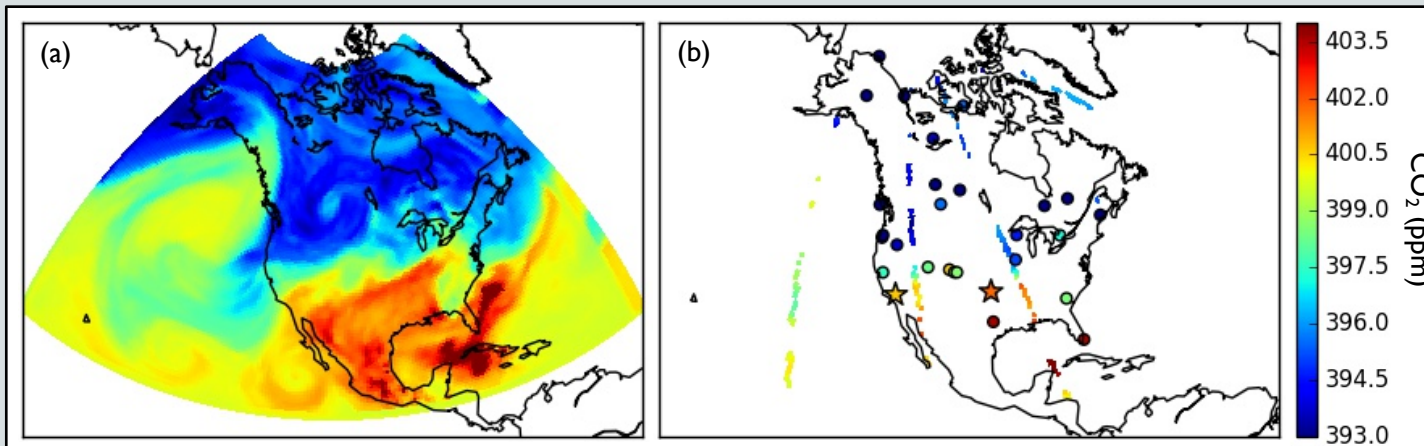


Figure 2. (a) Simulated XCO₂ and (b) measurements from flask and in situ sites (circles), TCCON (stars) and OCO-2 (tracks) over North America on 17 July 2015.

COMBINING SURFACE AND SPACE-BASED MEASUREMENTS

- Assimilating both surface- and space-based CO₂ measurements in a flux inversion fills in observational gaps.
- We performed a set of six-year flux inversions (2010-2015) assimilating CO₂ measurements from GLOBALVIEW+, TCCON, and ACOS b7.3 GOSAT (nadir only). Performed ensemble of inversions three times applying different prior NEE constraints (with no prior interannual variability).
- Posterior CO₂ fields were extensively evaluated against aircraft based CO₂ measurements and gave data-model differences similar to inversions assimilating surface-only or GOSAT-only observations (Byrne et al., 2019, ESSOAr, 2019; email me for latest version).

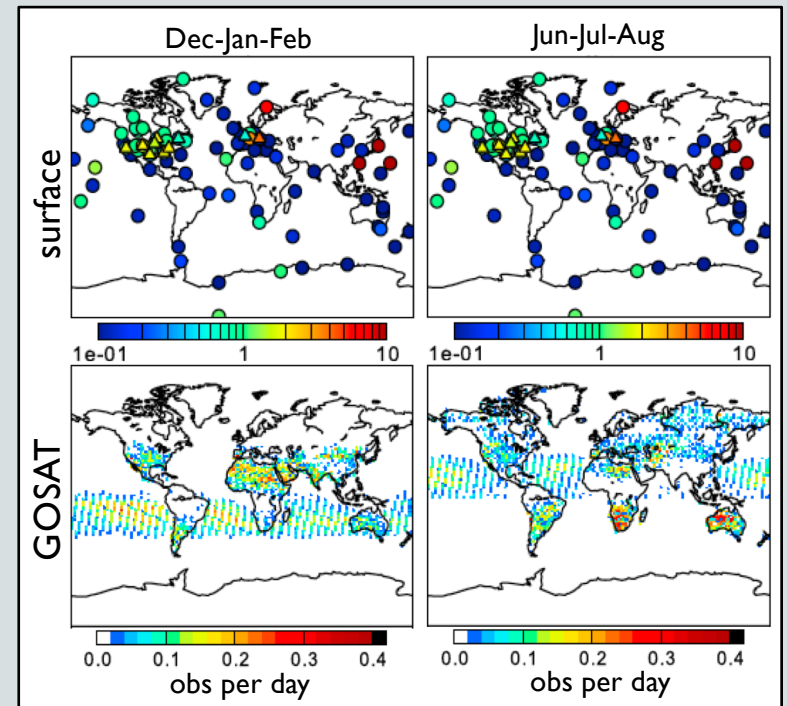


Figure 3. Number of measurements per day for surface-based (Obspack PROTOTYPE) and space-based (GOSAT) observing systems (Byrne et al., *JGR-A*, 2017).

INTERANNUAL VARIABILITY OVER NORTH AMERICA

- From the six-year posterior NEE fluxes we can examine the anomalies about a mean year:

$$\Delta NEE_{year} = NEE_{year} - \frac{1}{N} \sum_{i=0}^N NEE_i$$

- Inversions assimilating different combinations of datasets show differences in interannual variability (IAV).

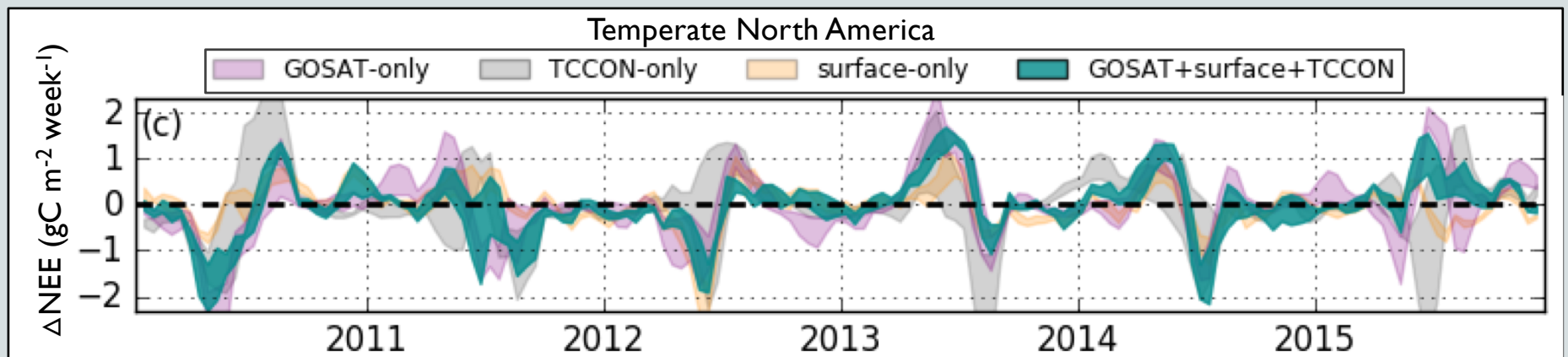


Figure 4. Two-week NEE anomalies over temperate North America for posterior NEE fluxes from inversions combining multiple datasets (green) and from inversions assimilating single datasets (Byrne et al., *ESSOAr*, 2019; email me for latest version).

INTERANNUAL VARIABILITY OVER NORTH AMERICA

- From the six-year posterior NEE fluxes we can examine the anomalies about a mean year:

$$\Delta NEE_{year} = NEE_{year} - \frac{1}{N} \sum_{i=0}^N NEE_i$$

- Inversions assimilating different combinations of datasets show differences in interannual variability (IAV).
- The combined inversion show seasonal compensation features.

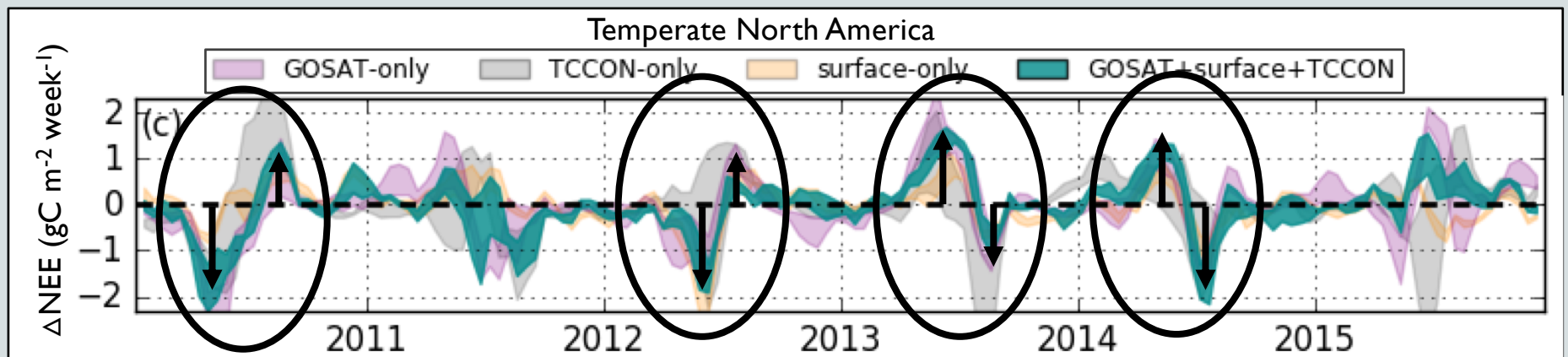


Figure 4. Two-week NEE anomalies over temperate North America for posterior NEE fluxes from inversions combining multiple datasets (green) and from inversions assimilating single datasets (Byrne et al., ESSOAr, 2019; email me for latest version).

SEASONAL COMPENSATION OBSERVED IN Δ GPP

- Studies have found seasonal cycle compensation in Δ GPP based on NDVI, SIF, flux tower, and phenology measurements.
- Does seasonal compensation in Δ NEE correspond to seasonal compensation in Δ GPP?

OPEN ACCESS

IOP PUBLISHING

Environ. Res. Lett. 8 (2013) 024027 (10pp)

ENVIRONMENTAL RESEARCH LETTERS

doi:10.1088/1748-9326/8/2/024027

Earlier springs decrease peak summer productivity in North American boreal forests

Wolfgang Buermann¹, Parida R Bikash², Martin Jung³, Donald H Burn⁴ and Markus Reichstein³

Research Article |  Open Access |   

Cropland Carbon Uptake Delayed and Reduced by 2019 Midwest Floods

Yi Yin , Brendan Byrne , Junjie Liu, Paul O. Wennberg, Kenneth J. Davis, Troy Magney, Philipp Köhler, Liyin He, Rupesh Jeyaram, Vincent Humphrey, Tobias Gerken, Sha Feng, Joshua P. Digangi, Christian Frankenberg ... [See fewer authors](#) 

The timing of autumn senescence is affected by the timing of spring phenology: implications for predictive models

TREVOR F. KEENAN¹ and ANDREW D. RICHARDSON²

¹Department of Biological Sciences, Macquarie University, Sydney, NSW 2109, Australia, ²Department of Organismic and Evolutionary Biology, Harvard University, Cambridge, MA 02138, USA

Widespread seasonal compensation effects of spring warming on northern plant productivity

Wolfgang Buermann^{1,2*}, Matthias Forkel³, Michael O'Sullivan¹, Stephen Stach⁴, Pierre Friedlingstein⁵, Vanessa Haverd⁶, Atul K. Jain⁷, Etsushi Kato⁸, Markus Kautz⁹, Sebastian Lienert^{10,11}, Danica Lombardozzi¹², Julia E. M. S. Nabel¹³, Hanqin Tian^{14,15}, Andrew J. Wiltshire¹⁶, Dan Zhu¹⁷, William K. Smith¹⁸ & Andrew D. Richardson^{19,20}

Satellite observations reveal seasonal redistribution of northern ecosystem productivity in response to interannual climate variability

Zachary Butterfield ^a , Wolfgang Buermann ^{b, c}, Gretchen Keppel-Aleks ^a

SEASONAL COMPENSATION AND AMPLIFICATION

- Examine six-year IAV in GOSAT+surface+TCCON posterior NEE (2010-2015) over North America.
- Examine 17-year of IAV in FluxSat GPP (2001-2017). FluxSat is a GPP product primarily using MODIS NBAR measurements and is calibrated using Fluxnet and SIF measurements (Joiner et al., 2018).

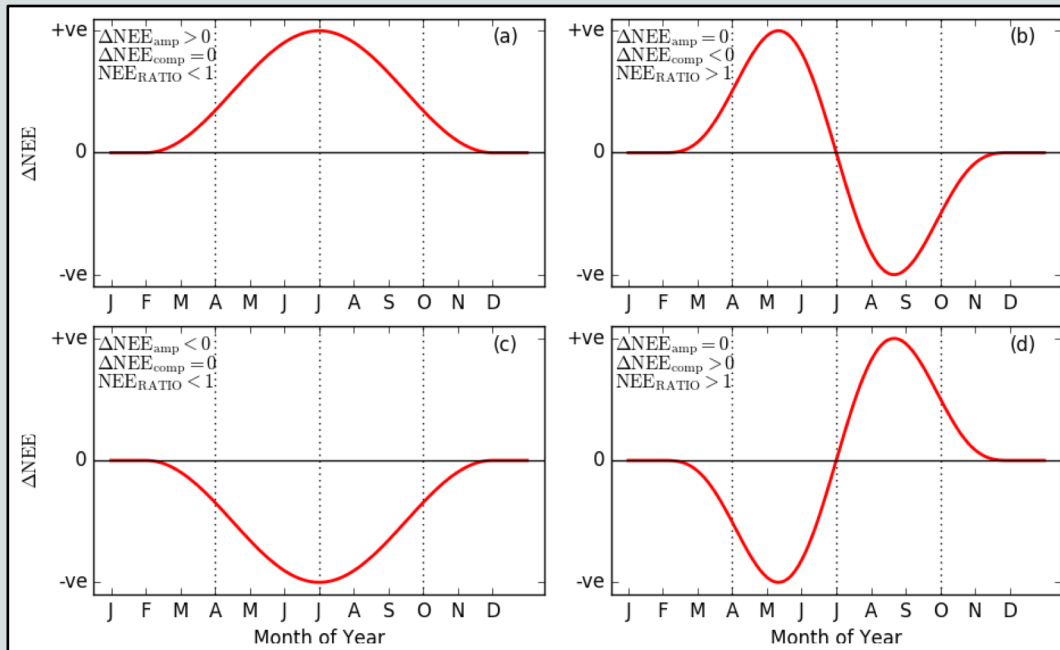


Figure 5. Illustration of amplification and compensation for NEE. (a) Positive amplification with no compensation, (b) no amplification with negative compensation, (c) negative amplification with no compensation, and (d) no amplification with positive compensation (Byrne et al., ESSOAr, 2020).

- Examine the relative magnitudes of amplification and compensation in IAV.

$$\begin{aligned} \Delta NEE_{\text{comp}} &= \Delta NEE_{\text{Jul-Aug-Sep}} - \Delta NEE_{\text{Apr-May-Jun}} \\ \Delta NEE_{\text{amp}} &= \Delta NEE_{\text{Jul-Aug-Sep}} + \Delta NEE_{\text{Apr-May-Jun}} \end{aligned}$$

$$NEE_{\text{RATIO}} = \frac{\sum_{y=2010}^{2015} |\Delta NEE_{\text{comp}}|}{\sum_{y=2010}^{2015} |\Delta NEE_{\text{amp}}|}$$

SEASONAL COMPENSATION OBSERVED IN GPP

- We do not expect the flux inversions to capture IAV on $4^{\circ} \times 5^{\circ}$ grid. This provides a first look at the general spatial structures in ΔGPP and ΔNEE .
- In general, amplification dominates in West/Southwest and compensation dominates in East/Northeast.

$$NEE_{RATIO} = \frac{\sum_{y=2010}^{2015} |\Delta NEE_{comp}|}{\sum_{y=2010}^{2015} |\Delta NEE_{amp}|}$$

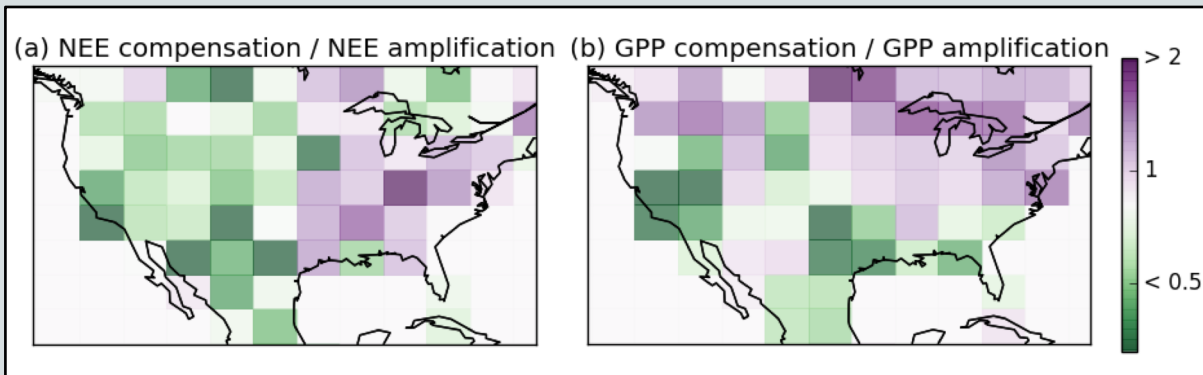


Figure 6. Relative magnitudes of seasonal compensation and amplification. (a) NEE_{RATIO} over 2010–2015 and (b) GPP_{RATIO} over 2001–2017 at $4^{\circ} \times 5^{\circ}$ spatial resolution (Byrne et al., ESSOAr, 2020).

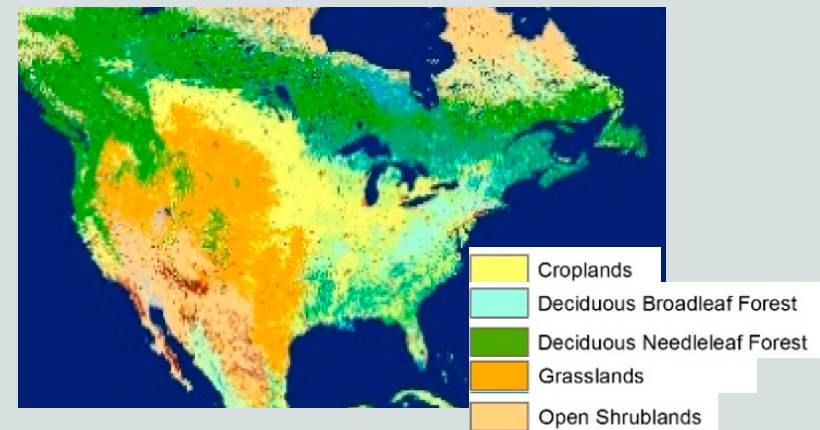


Figure 7. MODIS land cover types across North America

DOMINANT MODES OF IAV

- Singular value decomposition (SVD) of month-by-year array of anomalies show the dominant modes of variability between years.

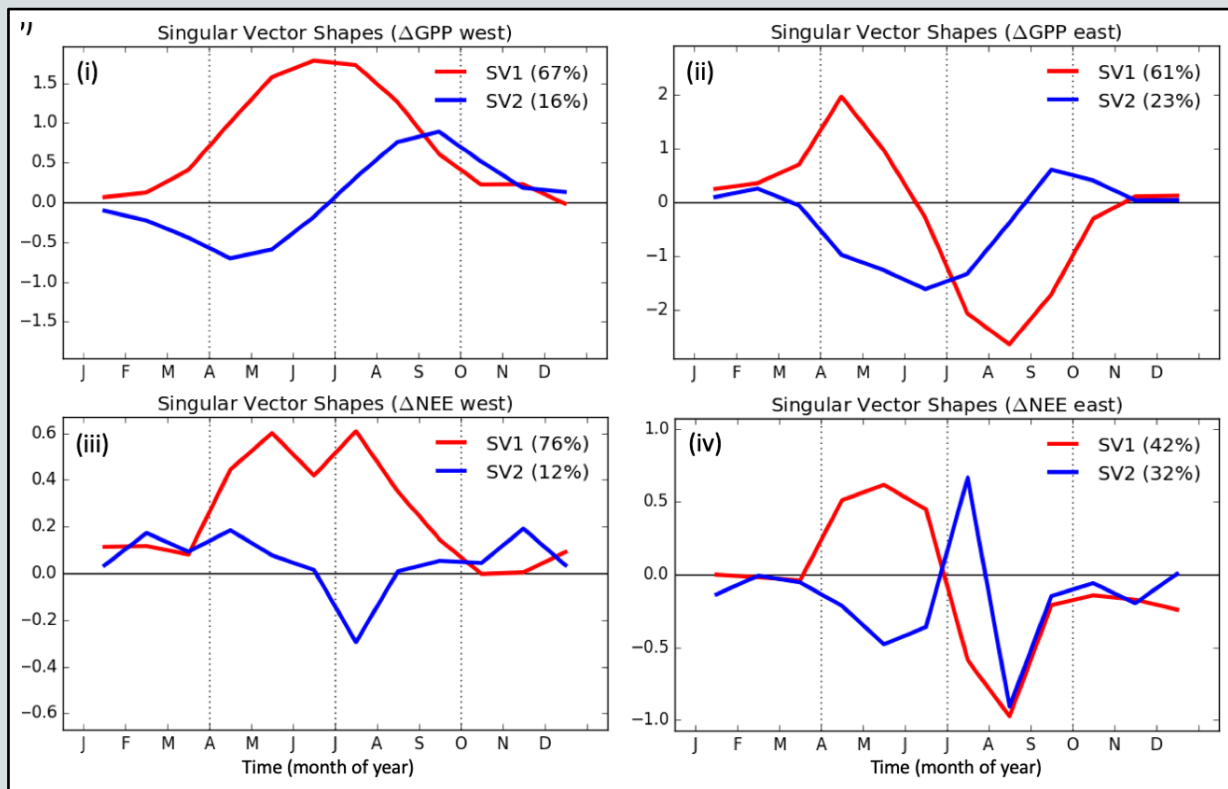


Figure 8. First and second singular vectors resulting from the decomposition of Δ GPP over 2001–2017 for the (i) western and (ii) eastern regions of North America, and Δ NEE over 2010–2015 for the (iii) western and (iv) eastern regions of North America (Byrne et al., ESSOAr, 2020).

- SVD analysis show that amplification dominates in the west and compensation dominates in the east for both Δ GPP and Δ NEE.

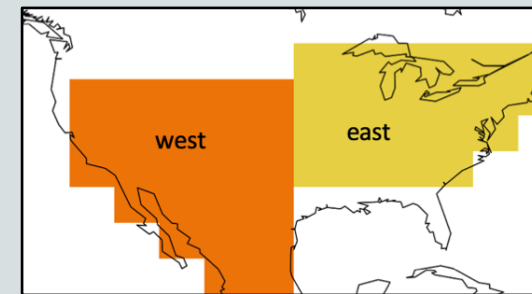
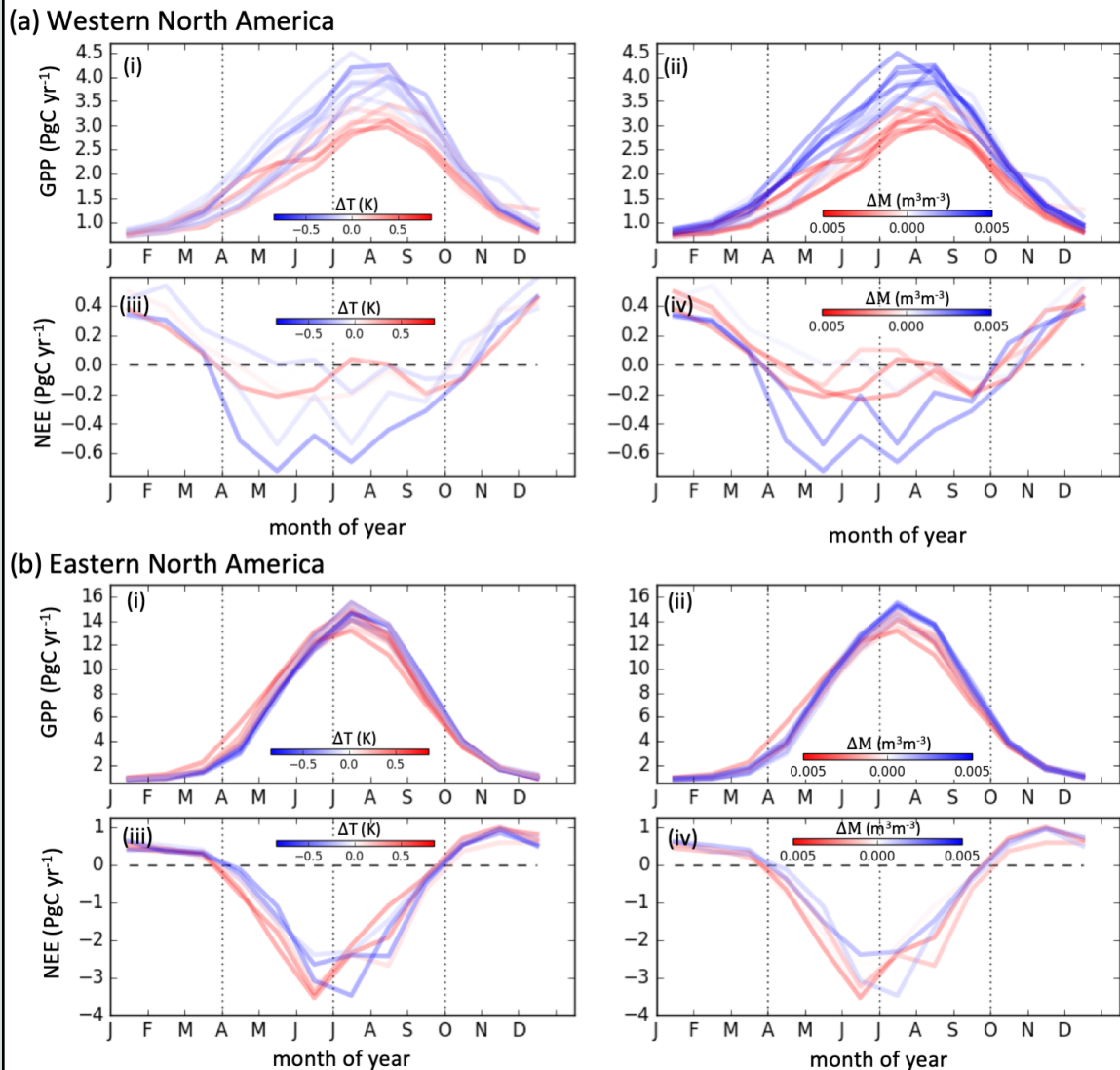


Figure 9. The spatial extent of western (orange) and eastern (yellow) regions of North America.

IAV IN CARBON FLUXES AND CLIMATE



- In West, amplification is associated with wetter-cooler conditions.
- In East, shift to earlier in the year is associated with warmer spring.
- These differences in IAV between the east and west result in a similar magnitude of annual net Δ GPP (104% of east) and Δ NEE (127% of east), in spite of larger annual mean GPP and NEE in the east. (Byrne et al., ESSOAr, 2020).

Figure 10. Seasonal cycles of GPP (2001–2017) and NEE (2010–2015) over eastern and western North America. (a) Seasonal cycles of (i-ii) GPP and (iii-iv) NEE over western North America. (b) Seasonal cycles of (i-ii) GPP and (iii-iv) NEE over eastern North America. Colors indicate the Apr-Sep ΔT ((i) and (iii)) or Apr-Sep ΔM ((ii) and (iv)) (Byrne et al., ESSOAr, 2020).

CONCLUSIONS

- Increasing observational coverage from surface- and space-based CO₂ observing systems are driving advances in our ability to detect changes in surface-atmosphere fluxes.
- NEE constrained by surface- and space-based CO₂ measurements suggest IAV in western North America is dominated by an amplification component while IAV in eastern North America is dominated by a compensation component.
- These results are supported by independent estimates of GPP IAV that give similar spatial and temporal variability.
- Both GPP and NEE suggest variability in the west is dominated by moisture availability, while variability in the east is most closely associated with temporal shifts in the seasonal cycle associated most closely with temperature.

ACKNOWLEDGMENTS

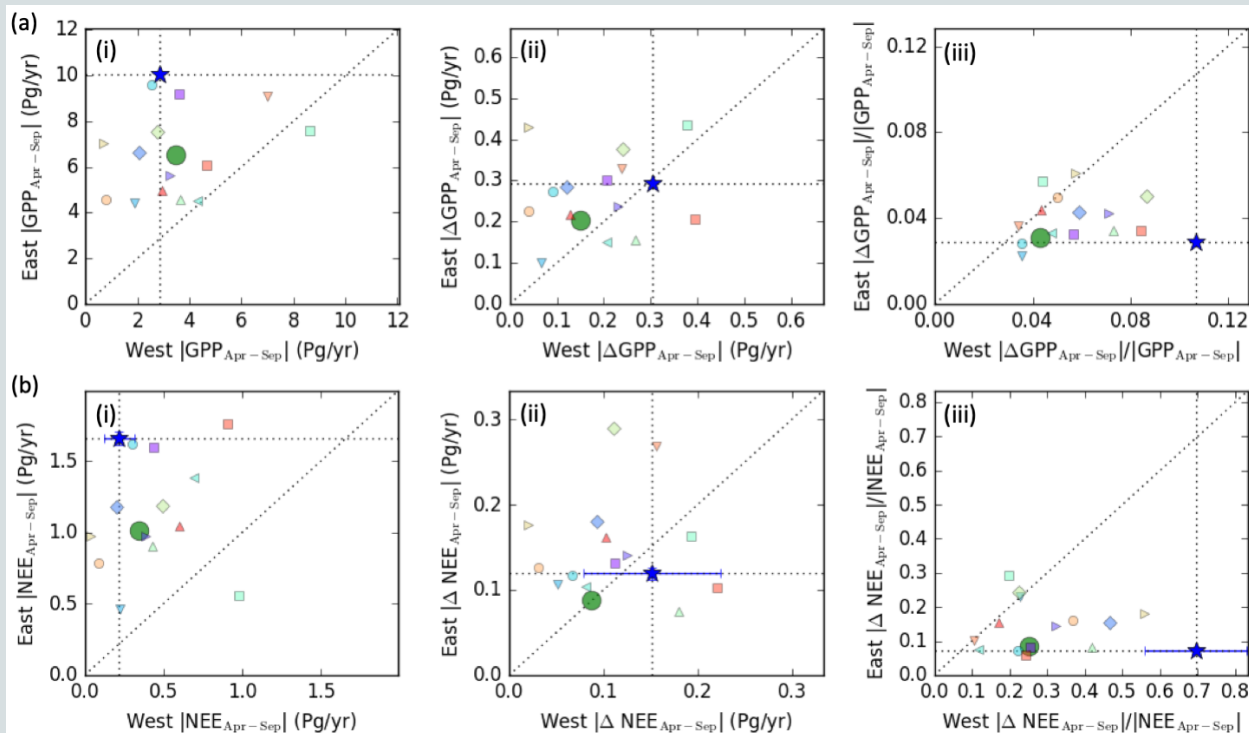
Brendan Byrne is supported by an appointment to the NASA Postdoctoral Program at the Jet Propulsion Laboratory, administered by Universities Space Research Association under contract with NASA. The research was carried out at the Jet Propulsion Laboratory, California Institute of Technology, under a contract with the National Aeronautics and Space Administration (80NM0018D004).

REFERENCES

- Byrne, B., Jones, D. B.A., Strong, K., Zeng, Z.-C., Deng, F., and Liu, J.: **Sensitivity of CO₂ Surface Flux Constraints to Observational Coverage**, J. Geophys. Res.-Atmos, 112, 6672–6694, <https://doi.org/10.1002/2016JD026164>, 2017.
- Byrne, B., Liu, J., Lee, M., Baker, I.T., Bowman, K.W., Deutscher, N. M., . . . Wunch, D.(2019). **Improved constraints on northern extratropical CO₂ fluxes obtained by combining surface-based and space-based atmospheric CO₂ measurements**. Earth and Space Science Open Archive. <https://doi.org/10.1002/essoar.10501108.2>
- Byrne, B., Liu, J., Bloom, A.A., Bowman, K.W., Butterfield, Z., Joiner, J., Keenan, T. F., Keppel-Aleks, G., Parazoo, N. C., Yin, Y. (2020).. **Outsized contribution of the semi-arid ecosystems to interannual variability in North American ecosystems**. Earth and Space Science Open Archive. <https://doi.org/10.1002/essoar.10502484.1>
- C. D. Keeling, S. C. Piper, R. B. Bacastow, M. Wahlen, T. P. Whorf, M. Heimann, and H.A. Meijer, **Exchanges of atmospheric CO₂ and ¹³CO₂ with the terrestrial biosphere and oceans from 1978 to 2000**. I. Global aspects, SIO Reference Series, No. 01-06, Scripps Institution of Oceanography, San Diego, 88 pages, 2001. <http://escholarship.org/uc/item/09v319r9>
- Joiner, J., Yoshida, Y., Zhang, Y., Duveiller, G., Jung, M., Lyapustin, A., et al. (2018). **Estimation of terrestrial global gross primary production (GPP) with satellite data-driven models and eddy covariance flux data**. Remote Sensing, 10(9), 1346. <https://doi.org/10.3390/rs10091346>

BACKUP – COMPARISON WITH MSTMIP

- Mean summer GPP and net uptake are larger in the east than the west (7.6x for GPP, 3.5x for NEE)
- However, Δ GPP and Δ NEE similar in the west and east (1.04x for GPP and 1.27x for NEE).
- Therefore, anomalies are a much larger fraction of the mean in the west.



- MsTMIP models show similar east/west differences.
- MsTMIP models tend to underestimate the magnitude of the anomalies in the west relative to the mean

Figure 11. Scatter plots of (a) GPP and (b) NEE fluxes in eastern and western North America. The panels show (i) the magnitude of Apr-Sep mean fluxes, (ii) the magnitude of Apr-Sep mean anomalies, and (iii) the ratio of the anomalies to mean fluxes. The blue star shows the observationally-based estimates from FluxSat GPP and the flux inversion NEE. The error bars on the observationally-constrained NEE estimate show the range in these values between the three flux inversions. The large green circle shows the GPP and NEE estimate from the MsTMIP model mean. Small circles show the GPP and NEE estimates from individual MsTMIP models.